Signatures of Majorana zero-modes in nanowires, quantum spin Hall edges, and quantum dots

Mi, S.

Author: Shuo Mi

Title: Signatures of Majorana zero-modes in nanowires, quantum spin Hall edges, and quantum dots

Issue Date: 2015-04-22

Chapter 1

Introduction

1.1 Preface

Majorana zero-modes, also referred to as *Majorana bound states* or *Majorinos*, are states in the middle of the excitation gap of a superconductor (so at zero excitation energy), bound to a magnetic vortex or other defect. The name goes back to a concept introduced by the Italian physicist Ettore Majorana [1], of a charge-neutral fermionic particle that is identical to its anti-particle. Such *Majorana fermions* may or may not be realized as fundamental particles in high energy physics, but in superconductors they appear naturally when a Cooper pair breaks up [2].

In field theory, particles that are their own anti-particles must be described by a real field, as the complex conjugate of a field creates the anti-particle. It is quite common for a bosonic particle to be described by a real field, the electromagnetic field of a photon being a familiar example. However, the field of a fermion is described by the Dirac equation, which is a complex wave equation. This led Paul Dirac to predict the existence of positrons as the anti-particles of electrons, given by a complex conjugate solution of his equation. What seemed to be a mathematical necessity was challenged in 1937 by Majorana, who showed that the Dirac equation allowed for real solutions. This opened up the possibility for the existence of charge-neutral fermions that would be their own anti-particle.

The search for Majorana fermions in particle physics focuses on the detection of the annihilation of pairs of neutrinos, to demonstrate the identity of neutrino and antineutrino [3]. But so far whether neutrinos are Majorana fermions is still an open question.

The situation is altogether different in superconductors: There Majorana fermions appear naturally as non-fundamental quasiparticles either localized or propagating inside specific solid state systems as a result of an unpaired electron can be seen equally well as a charge excess or a charge deficit of e. In an effective mean-field description the quasiparticle charge is therefore only conserved modulo $2e$, and this makes it possible to construct a coherent superposition of empty and filled states, i. e. electrons and holes, which is described by a real wave equation of the Majorana type. Pairs of superconducting quasiparticles, known as Bogoliubov quasipartiles which is a coherent supperposition of electrons and holes, can annihilate upon collision, demonstrating their Majorana nature [4].

Majorana fermions can be bound to a defect [5, 6]. The identity of particle and antiparticle then demands that this bound state is at zero energy, in the middle of the excitation gap. This socalled Majorana zero-mode is no longer a fermion, instead its statistics upon pairwise exchange depends on the order of the exchange operation [7]. Such non-Abelian statistics can be used to perform logical operations [8], an application known as topological quantum computation [9].

Although the earliest proposals to realize Majorana zero-modes in superconductors go back many decades [6, 7], these required an exotic form of pairing inside chiral p-wave superconductors. It was only realized recently that conventional s-wave pairing is sufficient in combination with spin-orbit coupling [10–13]. By now there is a great variety of systems in which Majorana zero-modes have been predicted [14–18], and there is mounting experimental evidence for their observation [19–23]. One such observation is shown in Figure 1.1 in a system of one dimensional semicondctor InSb nanowire with proximity to Nb superconducting reservoir.

In this thesis three platforms for Majorana zero-modes are investigated theoretically: one dimensional nanowires (Chapter 2), two dimensional topological insulators (Chapters 3, 4), and zero dimensional quantum dots (Chapters 5, 6). In this introductory chapter I will give an overview of the basic concept of a Majorana zero-mode, explaining the role played by superconductivity, followed by a discussion of identifying signatures and applications to quantum computation. Then a brief summary of each of the following chapters is given.

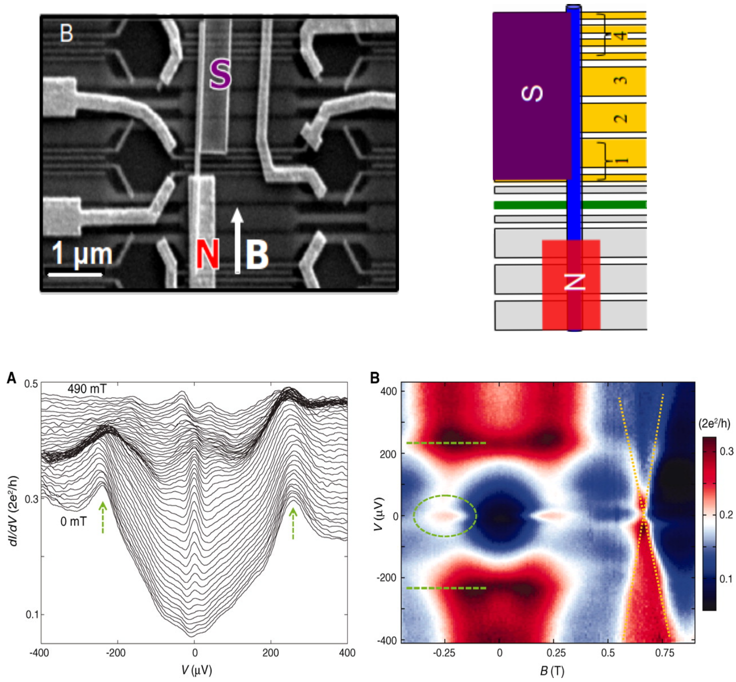

Figure 1.1. The first experimental observation of a Majorana zero-mode in a measurement of the differential conductance of an InSb nanowire coupled to a Nb superconductor. The zero-mode shows up as a zero-bias peak, emerging and persisting over a range of magnetic fields. Pictures taken from Ref. [19]. Reprinted with permission from AAAS.

1.2 The basics of Majorana zero-modes

1.2.1 The key role played by superconductivity

To construct a charge-neutral Majorana fermion in condensed matter one has to start with building blocks which are charged, electrons and holes. The hole is a vacancy state created below the Fermi level when an electron is excited above the Fermi sea. One can combine an electron and a hole to make a charge-neutral quasiparticle called an *exciton*. Since the exciton is a two-particle state combining a pair of half-integer-spin fermions, it is an integer-spin *boson*, like a photon.

To make a charge-neutral *fermion*, one needs to create a single-particle state as a coherent superposition of electron and hole. Such a coherent superposition requires a superconducting condensate. The idea is based on the understanding that the ground state of a superconductor is a collective condensate of pairs of electrons with opposite momentum and spin, socalled *Cooper pairs*. As illustrated in Fig. 1.2, an unpaired electron then differs from an unpaired hole by one Cooper pair. Scattering processes that convert an electron into a hole, known as Andreev scattering or Andreev reflection, preserve energy and momentum but charge, and switch spin bands. It then becomes possible by adding or removing a Cooper pair from the condensate without consuming extra energy. This coupling of electron and hole degrees of freedom makes it possible to create a coherent superposition of oppositely charged quasiparticles. This charge-neutral excitation, a socalled Bogoliubov quasiparticle, is the superconducting analogue of a Majorana fermion.

To go from a Majorana fermion to a Majorana zero-mode we need to confine the quasiparticle. Fig. 1.3 shows the spectrum of bound states, socalled Andreev levels, existing within the superconducting gap in the core of a magnetic vortex. Due to particle-hole symmetry, the energy spectrum is symmetric with respect to the Fermi level at $\varepsilon = 0$, halfway within the gap at $\pm\Delta$. In a conventional superconductor the zero-point motion prevents the appearance of a level at $\varepsilon = 0$. All levels then come in $\pm\varepsilon$ pairs. An unpaired level at $\varepsilon = 0$ appears in a topological superconductor. This zero-mode is pinned, and it cannot move up or down in energy without breaking particle-hole symmetry. Because it is at zero excitation energy, it is half-particle and half-hole, so it is its own antiparticle. Hence the name Majorana zero-mode.

1.2.2 Majorana operators

The properties of Majorana zero-modes are conveniently described in second quantization representation, in terms of identical creation and annihilation operators. To introduce these, we consider the simplest case of one fermionic state. It can be either an empty state $|0\rangle \equiv \binom{1}{0}$ or an occupied state $|1\rangle \equiv \binom{0}{1}$. We can define creation and annihilation operators by

$$c_1^\dagger = |1\rangle\langle 0| = \begin{pmatrix} 0 & 0 \\ 1 & 0 \end{pmatrix}, \quad c_1 = |0\rangle\langle 1| = \begin{pmatrix} 0 & 1 \\ 0 & 0 \end{pmatrix}. \tag{1.1}$$

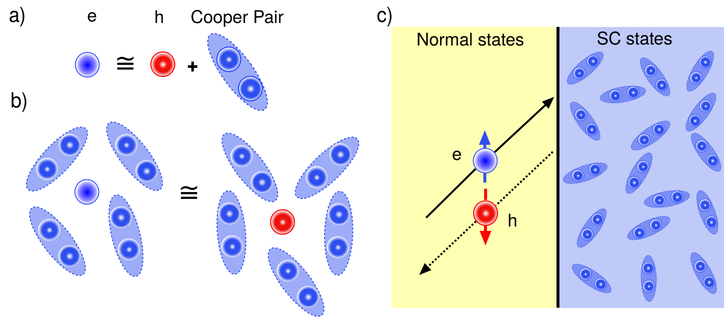

Figure 1.2. Panels (a) and (b) illustrate that an unpaired electron in a sea of Cooper pairs is equivalent to an unpaired hole. Panel (c) shows the conversion of an electron into a hole by Andreev reflection at the interface between a normal metal and a superconductor.

These operators satisfy fermionic anti-commutation relations,

$$\{c_i, c_j^\dagger\} = \delta_{ij}, \ \ \{c_i, c_j\} = \{c_i^\dagger, c_j^\dagger\} = 0. \tag{1.2}$$

Majorana operators are constructed from the creation and annihilation operators,

$$\gamma_1 = c_1 + c_1^\dagger = \begin{pmatrix} 0 & 1 \\ 1 & 0 \end{pmatrix} = \sigma_x, \tag{1.3}$$

$$\gamma_2 = -i(c_1 - c_1^\dagger) = \begin{pmatrix} 0 & -i \\ i & 0 \end{pmatrix} = \sigma_y, \tag{1.4}$$

$$c_1^\dagger = \frac{\gamma_1 - i\gamma_2}{2}, \ c_1 = \frac{\gamma_1 + i\gamma_2}{2}. \tag{1.5}$$

These are Hermitian operators, $\gamma_i = \gamma_i^\dagger$ ($\gamma_i^2 = \gamma_i^{\dagger 2} = 1$), obeying a modified anti-commutation relation:

$$\{\gamma_i, \gamma_j\} = 2\delta_{ij}. \tag{1.6}$$

In the terms of the Majorana operators the fermion number operator takes the form

$$\hat{\mathcal{N}} = c_1^\dagger c_1 = \frac{1 - i\gamma_2\gamma_1}{2}, \tag{1.7}$$

and the fermion parity operator is

$$\hat{\mathcal{P}} = i\gamma_2\gamma_1 = \sigma_z = (-1)^{\hat{\mathcal{N}}} = \mathrm{e}^{i\pi\hat{\mathcal{N}}} = \begin{pmatrix} 1 & 0 \\ 0 & -1 \end{pmatrix}. \tag{1.8}$$

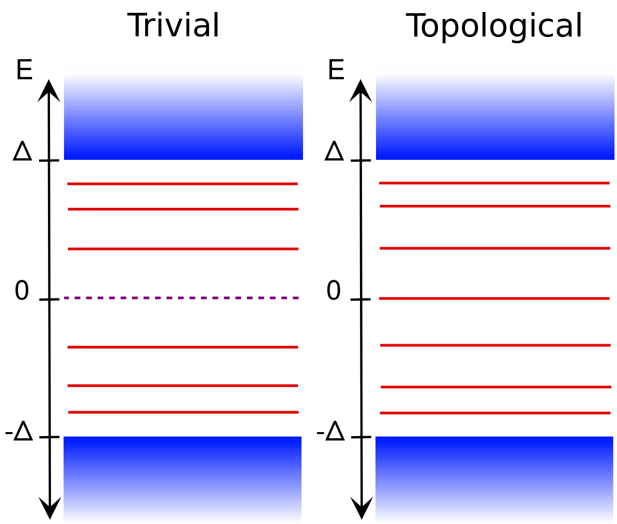

Figure 1.3. The distinction between the excitation spectrum of a conventional superconductor (left panel) and a topological superconductor (right panel). In both cases the spectrum has $\pm E$ symmetry, but the topological superconductor has an unpaired zero mode.

The fermion parity is $+1$ for the unoccupied state $|0\rangle$, and -1 for the occupied state $|1\rangle$. Note that $\{\gamma_i, \hat{\mathcal{P}}\} = 0$.

We may generalize this construction to an N-fermion state, giving rise to $2N$ Majorana operators,

$$\begin{aligned} \gamma_{2i-1} &= c_i + c_i^\dagger, \quad c_i^\dagger = \frac{\gamma_{2i-1} - i\gamma_{2i}}{2}, \\ \gamma_{2i} &= -i(c_i - c_i^\dagger), \quad c_i = \frac{\gamma_{2i-1} + i\gamma_{2i}}{2}. \end{aligned} \tag{1.9}$$

The corresponding fermion number and parity operators are given by

$$\hat{\mathcal{N}}_i = c_i^\dagger c_i = \frac{1 - i\gamma_{2i}\gamma_{2i-1}}{2}, \tag{1.10}$$

$$\hat{\mathcal{P}} = i\gamma_{2N}\gamma_{2N-1} \cdots i\gamma_2\gamma_1 = (-1)^{\sum_{i=1}^{N} \hat{\mathcal{N}}_i}. \tag{1.11}$$

It is worth to note that any Hamiltonian which is quadratic in the fermionic creation and annihilation operators preserves fermion parity, i. e. $[\hat{\mathcal{P}}, \hat{\mathcal{H}}] = 0$. Therefore, the Hilbert space of $2N$ Majorana operators divides into even and odd fermion number sectors, each of dimension 2^{N-1}.

1.2.3 Kitaev chain and Majorana zero-modes

As a simple example for the appearance of Majorana zero-modes, we now discuss the Kitaev chain model of a topological superconductor [24]. In this model the pair potential Δ involves electrons with the same spin on neighboring sites of the chain, so the spin degree of freedom can be ignored. Including also the nearest neighbor hopping energy t and chemical potential μ on N sites of the chain, the Hamiltonian is

$$H = \mu \sum_{i}^{N} c_i^\dagger c_i - \sum_{i=1}^{N-1} \left[t \left(c_i^\dagger c_{i+1} + c_{i+1}^\dagger c_i \right) + \Delta \left(c_i \, c_{i+1} + c_{i+1}^\dagger c_i^\dagger \right) \right]. \quad (1.12)$$

Upon Fourier transformation,

$$c_i = \frac{1}{\sqrt{N}} \sum_{k=-\infty}^{+\infty} \mathrm{e}^{-ik\cdot x_i} c_k, \; c_i^\dagger = \frac{1}{\sqrt{N}} \sum_{k=-\infty}^{+\infty} \mathrm{e}^{+ik\cdot x_i} c_k^\dagger, \quad (1.13)$$

the Hamiltonian can be rewritten in a matrix form in Nambu space,

$$H = \frac{1}{2} \sum_{k=0}^{\infty} \begin{pmatrix} c_k^\dagger & c_{-k} \end{pmatrix} h_{BdG} \begin{pmatrix} c_k \\ c_{-k}^\dagger \end{pmatrix}, \quad (1.14)$$

where h_{BdG} is the socalled Bogoliubov-de Gennes Hamiltonian. For the Kitaev model it has the form

$$h_{BdG} = (\mu - 2t\cos k)\tau_z + (2\Delta \sin k)\tau_y = \epsilon_k \tau_z + \Delta_k \tau_y = \mathbf{d} \cdot \boldsymbol{\tau}, \quad (1.15)$$

where $\mathbf{d} = (0, \Delta_k, \epsilon_k)$ and $\boldsymbol{\tau} = (\tau_x, \tau_y, \tau_z)$. The energy spectrum is given by $E_k = \pm\sqrt{\epsilon_k^2 + \Delta_k^2} = \pm|\mathbf{d}|$. When k runs over the Brillouin zone $k \in [0, 2\pi]$ the vector $\mathbf{d}(k)$ forms a closed loop winding around the origin an even number of times, i.e. the topologically trivial case, or an odd number of times, i.e. the topologically nontrivial case. The former corresponds to $|\mu| > |2t|$, while the latter corresponds to $|\mu| < |2t|$.

The topologically nontrivial case $|\mu| < |2t|$ has Majorana zero-modes at the end points of the chain. To see this, we transform from the

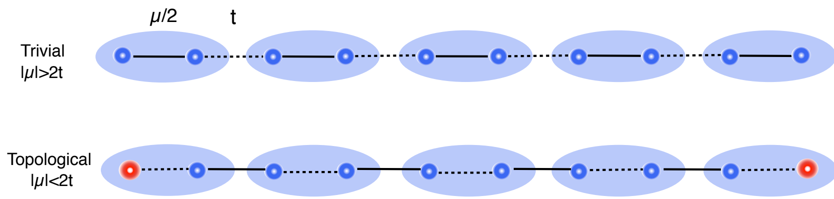

Figure 1.4. A schematic demonstration of the appearance of unpaired Majorana zero-modes (red dots) at the end points of the Kitaev chain. The shadow area indicates a site of the lattice, with a fermionic operator c_i represented by a pair of Majorana operators γ_{2i-1} and γ_{2i}.

operators c_n to the Majorana operators γ_n defined in Eq. (1.10),

$$\begin{aligned} H = \frac{\mu}{2} \sum_{n=1}^{N} (1 - i\gamma_{2n}\gamma_{2n-1}) \\ + i \sum_{n=1}^{N-1} \left[\frac{(\Delta + t)}{2} \gamma_{2n+2}\gamma_{2n-1} + \frac{(\Delta - t)}{2} \gamma_{2n+1}\gamma_{2n} \right]. \end{aligned} \tag{1.16}$$

For $t = -\Delta$, $\mu = 0$ the Hamiltonian simplifies to

$$H = \Delta \sum_{n=1}^{N-1} i\gamma_{2n+1}\gamma_{2n}. \tag{1.17}$$

The operators γ_1 and γ_{2N} do not appear in the Hamiltonian (1.17), and they commute with the Hamiltonian, i. e. $[\gamma_1, H] = [\gamma_{2N}, H] = 0$. These two unpaired Majorana operators define the *Majorana zero-modes*. They correspond to a fermion state $c = \frac{1}{2}(\gamma_1 + i\gamma_{2N})$ which splits over the two end points of the chain (see Fig. 1.4). In this topologically nontrivial case, the Hamiltonian has two degenerate ground states at zero energy, distinguished by the occupation number of the fermionic state. This degeneracy has been proposed by Kitaev as a way to store information in a quantum computer. Because the information is distributed over the two ends of the chain, it is believed to be less sensitive to external perturbations than information that is stored locally.

1.2.4 Experimental signatures

There exists a variety of experimental features that can serve as a "smoking gun" for the existence of Majorana zero-modes. The first experiments focused on the zero-bias peak of the tunnelling conductance. Due to perfect Andreev reflection at the zero-mode, the zero-temperature, zero-voltage limit of the differential conductance is quantized to $2e^2/h$ [25]. In the experiment [19], see Fig.1.1, the zero-bias conductance peak is an order of magnitude smaller, presumbaly because of thermal averaging. This complicates the unambiguous interpretation of the experiment, because there are other mechanisms that could give a non-quantized zero-bias peak [26, 27]. (One such mechanism is discussed in Chapter 5 of this thesis.)

Another feature of Majorana zero-modes is the so called 4π-periodic Josephson effect [10, 24, 28]. The energy spectrum of a Josephson junction containing a pair of Majorana zero-modes, separated by a tunnel barrier, is 4π-periodic in the phase difference ϕ across the junction. This corresponds to a flux periodicity of h/e, twice the usual $h/2e$ periodicity. One can understand the change from $2e$ to e as a manifestation of the fact that a Majorana fermion is only half an electron.

1.2.5 Non-Abelian statistics

Unlike Majorana fermions, which have the usual fermionic statistics (a sign change of the wave function upon pairwise exchange), the exchange statistics of Majorana zero-modes is non-Abelian, it depends on the order of the exchange operations [7].

Quite generally, for Abelian statistics the exchange of a pair of indistinguishable particles multiplies the wave function by a phase factor, $\psi \mapsto e^{i\theta}\psi$. The phase θ can be 0 (bosons), π (fermions) or any other value $\theta \in (0, \pi)$ (anyons). Different exchanges commute with each other.

For non-Abelian statistics the exchange operates on a manifold of degenerate states (all zero-modes are at $\varepsilon = 0$), mapping one state on another via a unitary transformation, $\psi \mapsto U\psi$. Because matrix multiplication does not commute, the order of the exchange operations matters. Specifically the exchange of two Majorana zero-modes i, j corresponds to an unitary operator $U(T_{ij})$ which is given by

$$U(T_{ij}) = \frac{1 - \gamma_i\gamma_j}{\sqrt{2}}, \;\; U(T_{ij})^\dagger = U(T_{ij})^{-1} = \frac{1 + \gamma_i\gamma_j}{\sqrt{2}}. \tag{1.18}$$

The Majorana operators transform as follows:

$$\begin{aligned} U(T_{ij})\gamma_i U(T_{ij})^\dagger &= \ \ \gamma_j, \\ U(T_{ij})\gamma_j U(T_{ij})^\dagger &= -\gamma_i, \\ U(T_{ij})\gamma_k U(T_{ij})^\dagger &= \ \ \gamma_k \quad (k \neq i,\, j). \end{aligned} \tag{1.19}$$

If we take three Majorana zero-modes $\{\gamma_i, \gamma_j, \gamma_k\}$ the pairwise exchanges $i \leftrightarrow j$ and $j \leftrightarrow k$ do not commute, because the two operators $U(T_{ij}) = (1 - \gamma_i\gamma_j)/\sqrt{2}$ and $U(T_{jk}) = (1 - \gamma_j\gamma_k)/\sqrt{2}$ do not commute, i. e. the commutator $[U(T_{ij}), U(T_{jk})] = \gamma_i\gamma_k$ is non-zero. Such non-commuting sequence of pairwise exchanges is called “braiding”.

Braiding of Majorana zero-modes is not sufficiently powerful to produce *all* logical operations, but a subset of operations can be obtained in this way [9]. Braiding is insensitive to local sources of decoherence, because it does not involve phase shifts as for ordinary unitary evolution of a quantum state. One says that the braiding operation has “topological protection”. Quantum computations assisted by braiding operations are called topological quantum computations.

1.3 This thesis

1.3.1 Chapter 2

To explain the experimental results in InSb nanowires achieved by the Delft group [19], we investigate whether the appearance of a soft gap in the differential conductance can be reconciled with the existence of Majorana zero-modes. From our simulation and calculation, we conclude that the combination of weak disorder with a partial coverage of the wire by the superconductor does indeed give rise to a softening of the induced superconducting gap. We find that the soft gap does not prohibit the presence of Majorana zero-modes, supporting an interpretation of the observed zero-bias conductance peak in these terms. We also point out that the minimal gap in such a nanowire is very small, thus it severely limits the lifetime of a Majorana qubit.

1.3.2 Chapter 3

The quantum spin Hall effect is an analogue of the quantum Hall effect in a system where time-reversal symmetry is not broken by a magnetic field [30–35]. The edge of a quantum spin Hall insulator has counterpropagating helical modes, with the direction of motion tied to the spin direction. As long as time-reversal symmetry is preserved, there can be no backscattering in the helical mode. When superconductivity is induced at the edge, a Majorana zero-mode is predicted to appear [10, 11]. The advantages of this system over the nanowire, are that the conduction happens in a single mode and that disorder cannot cause any backscattering. The disadvantage is that one cannot create an electrostatic barrier in this system, since the absence of backscattering prohibits that. A ferromagnetic insulator does form a tunnel barrier, but this material is experimentally inconvenient. As an alternative, we suggest a gate controllable metallic puddle with weak disorder and weak magnetic field to induce back scattering of the edge state. We show that the zero-bias peak from the Majorana zero-mode is hidden in a single conductance measurement, but is revealed upon averaging over gate voltages. Using this geometry as a building block, we design a flux-controlled circuit to perform a braiding operation.

1.3.3 Chapter 4

We continue our study of the quantum spin Hall effect, to explain a remarkable finding by the group from Rice University [36]: in InAs/GaSb quantum wells the helical edge conduction persists in perpendicular magnetic fields as large as 8 T, when we would expect strong backscattering from time-reversal symmetry breaking. We cannot quite explain the experimental data, but we do find an unusual phase diagram in our model calculation: The critical breakdown field for helical edge conduction splits into two fields with increasing disorder, an upper critical field for the transition into a quantum Hall insulator (supporting chiral edge conduction) and a lower critical field for the transition to bulk conduction in a quasi-metallic regime. The spatial separation of the inverted bands, typical for broken-gap InAs/GaSb quantum wells, is essential for the magnetic-field induced bulk conduction — there is no such regime in the HgTe quantum wells studied by the Würzburg group [34].

1.3.4 Chapter 5

The characteristic feature of the Delft experiment [19] is a resonant peak around zero bias-voltage V that does not split upon variation of a magnetic field B. In the $B - V$ plane the conductance peaks trace out an unusual Y-shaped profile, distinct from the more common X-shaped profile of peaks that meet and immediately split again. It is tempting to think that the absence of a splitting of the zero-bias conductance peak demonstrates unambiguously that the quasi-bound state is nondegenerate, hence Majorana. However, as found in Ref. [26], the Y-shaped conductance profile is generic for superconductors with broken spin-rotation symmetry and broken time-reversal symmetry, irrespective of the presence or absence of Majorana zero-modes. In this chapter we investigate the appearance of such "fake Majorana peaks" in the framework of random-matrix theory. We contrast the two ensembles with broken time-reversal symmetry, in the presence of spin-rotation symmetry (symmetry class C), or in its absence (class D). The poles of the scattering matrix in the complex plane, encoding the center and width of the resonance, are repelled from the imaginary axis in class C, but attracted to it in class D. This explains the appearance of Andreev resonances that are are pinned to the middle of the gap and produce a zero-bias conductance peak that does not split over a range of parameter values (Y-shaped profile).

1.3.5 Chapter 6

In this chapter, we demonstrate how the superconducting phase difference in a Josephson junction may be used to remove the Kramers degeneracy of the Andreev levels, producing a nondegenerate two-level system that can be used as a qubit for quantum information processing. The splitting is known to be small in two-terminal Josephson junctions, but when there are three or more terminals the splitting becomes comparable to the superconducting gap. Application of a phase difference can then cause the switch of the ground state fermion parity from even to odd, observed as a crossing of the Andreev levels at the Fermi energy. In essence, the multi-terminal Josephson junction realizes a "discrete vortex" in the junction, which may eventually be used to trap Majorana zero-modes.

Bibliography

[1] E. Majorana, Nuovo Cimento **5**, 171 (1937).

[2] F. Wilczek, Nature Physics **5**, 614 (2009).

[3] S. R. Elliott and M. Franz, arXiv:1403.4976.

[4] C. W. J. Beenakker, Phys. Rev. Lett. **112**, 070604 (2014).

[5] N. B. Kopnin and M. M. Salomaa, Phys. Rev. B **44**, 9667 (1991).

[6] G. E. Volovik, JETP Letters **70**, 609 (1999).

[7] N. Read and D. Green, Phys. Rev. B **61**, 10267 (2000).

[8] S. B. Bravyi and A. Yu. Kitaev, Ann. Phys. **298**, 210 (2002).

[9] C. Nayak, S. H. Simon, A. Stern, M. Freedman, and S. Das Sarma, Rev. Mod. Phys. **80**, 1083 (2008).

[10] L. Fu and C. L. Kane, Phys. Rev. Lett. **100**, 096407 (2008).

[11] L. Fu and C. L. Kane, Phys. Rev. B **79**, 161408(R) (2009).

[12] R. Lutchyn, J. Sau, and S. Das Sarma, Phys. Rev. Lett. **105**, 077001 (2010).

[13] Y. Oreg, G. Refael, and F. von Oppen, Phys. Rev. Lett. **105**, 177002 (2010).

[14] M. Z. Hasan and C. L. Kane, Rev. Mod. Phys. **82**, 3045 (2010).

[15] X.-L Qi and S. C. Zhang, Rev. Mod. Phys. **83**, 1057 (2011).

[16] J. Alicea, Rep. Prog. Phys. **75**, 076501 (2012).

[17] C. W. J. Beenakker, Ann. Rev. Cond. Mat. Phys. **4**, 113 (2013).

[18] J. Alicea and A. Stern, arXiv:1410.0359.

[19] V. Mourik, K. Zuo, S. M. Frolov, S. R. Plissard, E. P. A. M. Bakkers, and L. P. Kouwenhoven, Science **336**, 1003 (2012).

[20] M. T. Deng, C. L. Yu, G. Y. Huang, M Larsson, P. Caroff, and H. Q. Xu, Nano Lett. **12**, 6414 (2012).

[21] H. A. Nilsson, P. Samuelsson, P. Caroff, and H. Q. Xu, Nano Lett. **12**, 228 (2012).

[22] A. Das, Y. Ronen, Y. Most, Y. Oreg, M. Heiblum, and H. Shtrikman, Nature Phys. **8**, 887 (2012).

[23] S. Nadj-Perge, I. K. Drozdov, J. Li, H. Chen, S. Jeon, J. Seo, A. H. MacDonald, B. A. Bernevig, and A. Yazdani, Science **346**, 602 (2014).

[24] A. Yu. Kitaev, Phys.-Usp. **44**, 131 (2001).

[25] K. T. Law, P. A. Lee, and T. K. Ng, Phys. Rev. Lett. **103**, 237001 (2009).

[26] D. I. Pikulin, J. P. Dahlhaus, M. Wimmer, H. Schomerus, and C. W. J. Beenakker, New J. Phys. **14**, 125011 (2012).

[27] J. Liu, A. C. Potter, K. T. Law, and P. A. Lee, Phys. Rev. Lett. **109**, 267002 (2012).

[28] L. P. Rokhinson, X. Liu, and J. K. Furdyna, Nat. Phys. **8**, 795 (2012).

[29] A. Stern and N. H. Lindner, Science **339**, 1179 (2013).

[30] C. L. Kane and E. J. Mele, Phys. Rev. Lett. **95**, 226801 (2005).

[31] B. A. Bernevig and S. C. Zhang, Phys. Rev. Lett. **96**, 106802 (2006).

[32] B. A. Bernevig, T. L. Hughes and S. C. Zhang, Science **314**, 1757 (2006).

[33] C. X. Liu, T. L. Hughes, X. -L. Qi, K. Wang, and S. C. Zhang, Phys. Rev. Lett. **100**, 236601 (2008).

[34] M. König, S. Wiedmann, C. Brüne, A. Roth, H. Buhmann, L. W. Molenkamp, X. -L. Qi, and S. C. Zhang, Science, **318**, 5851 (2007).

[35] M. König, H. Buhmann, L. W. Molenkamp, T. L. Hughes, C. -X. Liu, X. -L. Qi, and S. C. Zhang, J. Phys. Soc. Jpn. **77**, 031007 (2008).

[36] L. Du, I. Knez, G. Sullivan, and R.-R. Du, arXiv:1306.1925